

Reference Voltage Optimization of a Hybrid Filter for Nonlinear Load Compensation

Salvador P. Litrán and Patricio Salmerón

Abstract—The harmonic problem in electric power systems, far from improving, has been increasing in recent years. To mitigate this problem, active filters have been proposed; however, they do not present a complete solution for any type of load and system. This paper develops a control strategy for a compensator based on a hybrid filter topology. This topology is formed by an active power filter of series connection and a passive filter of parallel connection. The proposed strategy is based on minimizing the root-mean-square value of the voltage at the point of common coupling so that the source transfers the power demanded by the load. Thus, the determination of the reference signal is posed as a constrained optimization problem. The strategy was proposed for four- and three-wire systems, and it allowed the compensation of current harmonics and reactive power of harmonic current source and harmonic voltage source loads. An experimental prototype was developed, which has allowed verification of their performance.

Index Terms—Active filter, electric power quality, harmonics, hybrid filter.

I. INTRODUCTION

NOWADAYS, power quality is a growing problem in power systems. This is mainly due to the increased use of power electronic components within the distribution system and the reliance on renewable energy sources which have converters as interface between the source and the power system. On the other hand, new technical and legislative developments shape the electricity market, whereby the reliability of power systems and the profitability of utility companies must be maintained. Therefore, one of the main responsibilities of a utility system is to supply electric power in the form of sinusoidal voltages and currents with appropriate magnitudes and frequency for the customers at the point of common coupling (PCC). However, the presence of nonlinear loads distorts the voltage and current waveforms, causing the appearance of harmonics [1]. The major issues associated with the nonlinear load harmonics are severe overheating: Increased operating temperatures of generators and transformers degrade the insulation material of their windings.

To optimize the performance and stability of power systems and to overcome power quality problems, many techniques

and devices have been proposed and implemented. Several approaches are based on power electronic devices [2] that offer a variety of options including series and shunt active filters and reactive power compensation to improve power quality [3]–[8]. Therefore, installation of active power filters (APFs) proves indispensable for solving power quality problems in distribution networks such as the compensation of current and voltage harmonics, reactive power, voltage sags, voltage flicker, and negative and zero-phase sequence currents.

Most of the APFs that have been implemented now are of shunt type. A major drawback of active filters is their high rating. Due to it and cost considerations, the acceptability of active filters has been limited in practical applications. They are comparatively more expensive due to their large rating of about 30%–60% of the load [5], [6].

In response to these factors, different structures of hybrid filters have evolved as a cost-effective solution for the compensation of nonlinear loads [9]–[16]. Hybrid filters combine a number of passive and/or active filters, and their structure may be of series or parallel topology or a combination of the two. Hybrid filters are found to be more effective in providing complete compensation of various types of nonlinear loads. The advantages of hybrid topologies are quite significant since the series APF can be very low rated, between 3% and 10%, and the disadvantages of passive filters are mitigated.

One of these hybrid filter topologies is based on an active filter in series with the source and a passive filter in parallel with the load (SAPPF) [14]–[17]. The passive circuit performs basic filtering action at the dominant harmonic frequencies (e.g., fifth or seventh), whereas the active elements, through precise control, mitigate higher harmonics. This will effectively reduce the overall size and cost of active filtering.

For this configuration, various control strategies have been proposed for the active filter. Some are aimed at eliminating current harmonics, improving the behavior of the passive filter [14]–[16]. Others additionally compensate the reactive power. In the latter case, the calculation algorithm is based on the formulation of the instantaneous reactive power [18], [19] in order to achieve constant power on the side source when it is applied to a balanced, three-phase, and three-wire system. Similar compensation objectives are proposed in [17], where the control strategy is based on the dual vectorial formulation of the instantaneous reactive power. This strategy is applicable to unbalanced three-phase four-wire systems, and it allows the reactive power to be compensated and the source current harmonics to be eliminated.

This paper develops a control strategy for SAPPF, which is based on minimizing the effective value of the voltage at the

Manuscript received February 7, 2013; revised May 28, 2013; accepted July 16, 2013. Date of publication July 31, 2013; date of current version December 20, 2013. This work was supported by the “Ministerio de Economía y Competitividad” of the Government of Spain under Grant DPI2010-17709.

The authors are with the Department of Electrical Engineering, Escuela Técnica Superior de Ingeniería, University of Huelva, 21819 Huelva, Spain (e-mail: salvador@uhu.es; patricio@uhu.es).

Color versions of one or more of the figures in this paper are available online at <http://ieeexplore.ieee.org>.

Digital Object Identifier 10.1109/TIE.2013.2276078

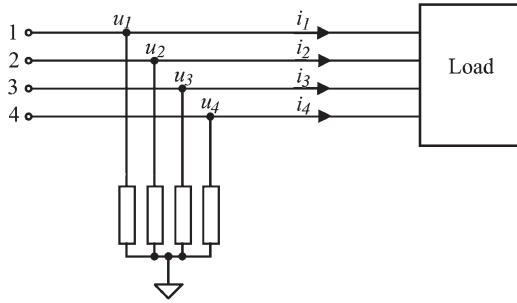


Fig. 1. Four-wire system.

PCC to ensure the transfer of the power demanded by the load. Thus, the determination of the reference signal is raised as a problem of constrained optimization to systems of three and four wires. This allows harmonic mitigation and reactive power compensation.

The proposed strategy was applied to an experimental prototype of hybrid filter which has allowed verification of their performance in the compensation of harmonic current source (HCS) and harmonic voltage source (HVS) nonlinear loads, with three and four wires.

II. COMPENSATION REFERENCE VOLTAGES

This section presents a compensation method based on the average value. The aim is to determine the minimum root-mean-square (rms) value of the voltage at the PCC so that the system transfers the active power to the load. To develop this strategy, a polyphase system is considered as a special case of multiconductor system [20]. Thus, a four-wire three-phase system can be represented by means of a multiconductor system as Fig. 1 shows.

The currents i_1 , i_2 , i_3 , and i_4 are the components of the line current vector, which is defined by

$$\mathbf{i} = [i_1 \quad i_2 \quad i_3 \quad i_4]^T. \quad (1)$$

As a consequence of Kirchhoff's current law, for the current vector \mathbf{i} is satisfied that

$$[1 \quad 1 \quad 1 \quad 1][i_1 \quad i_2 \quad i_3 \quad i_4]^T = 0. \quad (2)$$

Therefore, one of the components can always be expressed as a linear combination of the others. From the mathematical point of view, only $4 - 1$ components are sufficient to describe the current vector. However, in four-wire three-phase systems, the use of the four current components permits a direct description of the system behavior.

The system voltages may be defined with respect to a virtual neutral point. This corresponds to the neutral of a star formed by four impedances of the same value, as it is shown in Fig. 1.

In this way, it is possible to define the voltages u_1 , u_2 , u_3 , and u_4 of each of the conductors with respect to this common point. These voltages are the components of the voltage vector \mathbf{u} , which is defined by means of

$$\mathbf{u} = [u_1 \quad u_2 \quad u_3 \quad u_4]^T. \quad (3)$$

The four components of the voltage vector must verify that

$$[1 \quad 1 \quad 1 \quad 1][u_1 \quad u_2 \quad u_3 \quad u_4]^T = 0. \quad (4)$$

In what follows, the subscript Σ is used to refer to these "collective" values, including the fourth wire.

For a four-wire system, the instantaneous power is obtained by the scalar product of the voltage vector by the current vector which is expressed by the equation

$$p_\Sigma = \mathbf{u}^T \cdot \mathbf{i}. \quad (5)$$

In steady-state and periodic conditions, the average value of the instantaneous active power and the rms values of the voltage vector and current vector are defined for a fundamental period T . Thus, in regular conditions for an observation interval T corresponding to one period or a multiple of the period, the rms value is given by

$$U_\Sigma = \sqrt{\|\mathbf{u}\|^2} = \sqrt{\frac{1}{T} \int_t^{t+T} \left(\sum_{j=1}^4 u_j^2 \right) dt} = \sqrt{\sum_{j=1}^4 U_j^2}. \quad (6)$$

Here, U_j is the rms value of the j component of the voltage vector. In the same way, for the current vector given in (1), the rms value is defined by

$$I_\Sigma = \sqrt{\|\mathbf{i}\|^2} = \sqrt{\frac{1}{T} \int_t^{t+T} \left(\sum_{j=1}^4 i_j^2 \right) dt} = \sqrt{\sum_{j=1}^4 I_j^2} \quad (7)$$

where I_j is the rms value of the j component of the current vector.

The active power is obtained when the average value of the instantaneous power given in (5) is determined. Thus, for the fundamental period T , the active power is given by

$$P_\Sigma = \frac{1}{T} \int_t^{t+T} p_\Sigma dt. \quad (8)$$

On the other hand, the voltage vector \mathbf{u} can be determined such that the system transfers the power demanded by the load with minimum rms. To solve this optimization problem, the technique of Lagrange multipliers is used. Therefore, the objective function is defined by

$$F = \frac{1}{T} \int_t^{t+T} \mathbf{u} \cdot \mathbf{u} dt \quad (9)$$

subject to the constraint

$$G = \frac{1}{T} \int_t^{t+T} \mathbf{u} \cdot \mathbf{i} dt = P_\Sigma. \quad (10)$$

With the F and G functions defined in (9) and (10), respectively, the Lagrangian equation is expressed as

$$L = F + \lambda G. \quad (11)$$

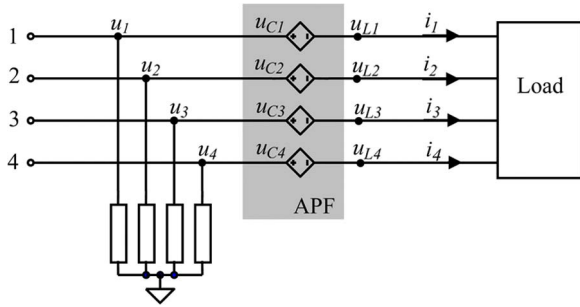


Fig. 2. Four-wire system with series compensation equipment.

Applying

$$\begin{aligned} \frac{\partial L}{\partial \mathbf{u}} &= 0 \\ \frac{\partial L}{\partial \lambda} &= 0 \end{aligned} \quad (12)$$

the result is an equation system whose solution is

$$\mathbf{u} = R \cdot \mathbf{i} \quad (13)$$

where R is given by the ratio between the average power and the rms value of the current

$$R = \frac{P_{\Sigma}}{I_{\Sigma}^2}. \quad (14)$$

Here, R represents the value of a resistive three-phase load, which transfers the same active power as the load. The application of (13) allows the determination of the voltage vector \mathbf{u} . These voltages applied to a symmetrical resistive load of resistance R transfer the same average power as the nonlinear load. In this way, it is achieved that, from the PCC, the system presents a unity power factor.

Fig. 2 shows a system of four wires compensated by means of a series APF. This is represented by four controlled voltage sources with values u_{C1} , u_{C2} , u_{C3} , and u_{C4} . These four components make up the compensation voltage vector defined by

$$\mathbf{u}_C = [u_{C1} \ u_{C2} \ u_{C3} \ u_{C4}]^T. \quad (15)$$

When Kirchhoff's voltage law is applied to the circuit in Fig. 2, it provides for the compensation voltage \mathbf{u}_C the relationship

$$\mathbf{u}_C = \mathbf{u} - \mathbf{u}_L \quad (16)$$

where \mathbf{u}_L is the load voltage vector. Taking into account (13) and (14), it results in

$$\mathbf{u}_C = \frac{P_{\Sigma}}{I_{\Sigma}^2} \mathbf{i} - \mathbf{u}_L. \quad (17)$$

Furthermore, it is possible to obtain the average power transferred by the compensator. For this purpose, (17) is multiplied by the current vector. If the resulting expression is integrated

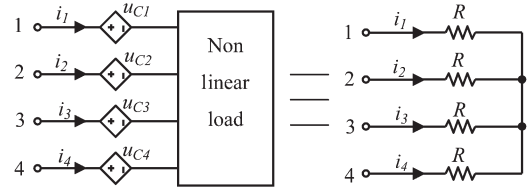


Fig. 3. Resistive behavior of the series APF and load.

over the period T , the system power balance is obtained; this is

$$\frac{1}{T} \int_t^{t+T} \mathbf{u}_C \cdot \mathbf{i} dt = \frac{1}{T} \int_t^{t+T} \frac{P_{\Sigma}}{I_{\Sigma}^2} \mathbf{i} \cdot \mathbf{i} dt - \frac{1}{T} \int_t^{t+T} \mathbf{u}_L \cdot \mathbf{i} dt. \quad (18)$$

The first term is the average power of the compensator, so that (18) can be rewritten as

$$P_{C\Sigma} = \frac{1}{T} \int_t^{t+T} \frac{P_{\Sigma}}{I_{\Sigma}^2} \mathbf{i} \cdot \mathbf{i} dt - \frac{1}{T} \int_t^{t+T} \mathbf{u}_L \cdot \mathbf{i} dt. \quad (19)$$

The first term in (19) constitutes the active power consumed by the resistor R , and the second term constitutes the load average power $P_{L\Sigma}$, which can be expressed by

$$P_{C\Sigma} = \frac{P_{\Sigma}}{I_{\Sigma}^2} \frac{1}{T} \int_t^{t+T} \mathbf{i} \cdot \mathbf{i} dt - P_{L\Sigma}. \quad (20)$$

Considering (7) and (14), (20) can be set as

$$P_{C\Sigma} = RI_{\Sigma}^2 - P_{L\Sigma} = P_{\Sigma} - P_{L\Sigma}. \quad (21)$$

Expression (21) represents the power balance of the compensated system. The average power transferred by the compensator must be zero; then,

$$P_{\Sigma} = P_{L\Sigma}. \quad (22)$$

The equality (22) allows the numerator of (14) to be identified as the average power load

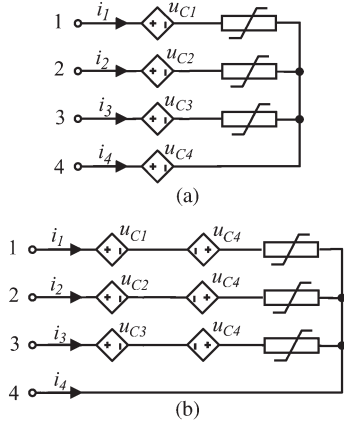
$$R = \frac{P_{L\Sigma}}{I_{\Sigma}^2}. \quad (23)$$

Thus, the compensation voltage vector defined in (17) must be expressed in terms of the average power of the load; this is

$$\mathbf{u}_C = \frac{P_{L\Sigma}}{I_{\Sigma}^2} \mathbf{i} - \mathbf{u}_L. \quad (24)$$

On the other hand, the application of (24) requires an inverter of four branches for four-wire systems. The use of this type of configuration has a higher cost and an added complication in the control circuit. In what follows, a simplification of the control strategy will be carried out, allowing the use of a converter of three branches.

The compensation strategy defined in (24) is based on the set APF/load behaves as a symmetrical resistive load (R) as it is shown in Fig. 3. The set of four resistors connected in star represents the optimum load. This load has the same structure

Fig. 4. Correction of the compensation voltage when $i_4 \neq 0$.

and the same voltage set as the load connected in star which defines the virtual neutral in Fig. 2.

Moreover, an unbalanced nonlinear load can be represented by means of three nonlinear branches connected between the phase and neutral as Fig. 4(a) shows. In this figure, according to (24), the following equations are obtained:

$$\begin{aligned} u_{C1} &= \frac{P_{L\Sigma}}{I_{\Sigma}^2} i_1 - u_{L1} \\ &\vdots \\ u_{C4} &= \frac{P_{L\Sigma}}{I_{\Sigma}^2} i_4 - u_{L4}. \end{aligned} \quad (25)$$

When the source u_{C4} is displaced to the branches 1, 2, and 3, the scheme shown in Fig. 4(b) is obtained. Then, the set of compensation voltages is

$$\begin{aligned} u'_{C1} &= u_{C1} - u_{C4} = \frac{P_{L\Sigma}}{I_{\Sigma}^2} (i_1 - i_4) - u_{L4} \\ u'_{C2} &= u_{C2} - u_{C4} = \frac{P_{L\Sigma}}{I_{\Sigma}^2} (i_2 - i_4) - u_{L4} \\ u'_{C3} &= u_{C3} - u_{C4} = \frac{P_{L\Sigma}}{I_{\Sigma}^2} (i_3 - i_4) - u_{L4}. \end{aligned} \quad (26)$$

Thus, the expressions (26) allow determining the compensation voltages for an APF constituted by three branches for any situation of the supply voltage.

III. EXPERIMENTAL PROTOTYPE

Fig. 5 shows the power circuit with the hybrid compensator. The active filter consists of three modules Semikron insulated-gate bipolar transistors (IGBTs) SKM50GB123 model, with three drivers SKHI 22A from the same manufacturer. At the dc side, the inverter has two capacitors of 2200 μF which are charged to 100 V. At the ac side of the inverter is connected a ripple LC filter formed by an inductor of 0.13 mH and a capacitor of 50 μF whose function is to eliminate high-frequency components due to the switching of power devices.

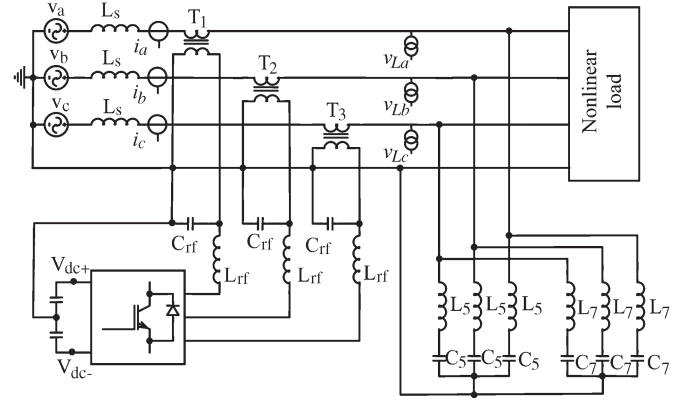


Fig. 5. Experimental prototype scheme of the hybrid filter.

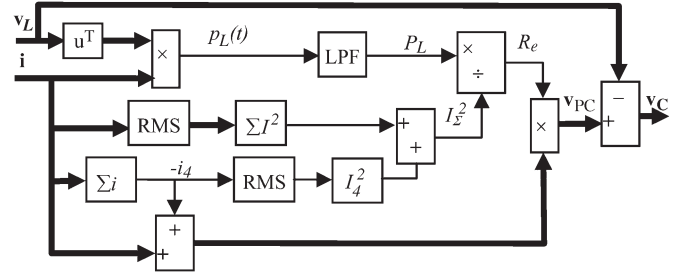


Fig. 6. Block scheme to determine the compensation voltage.

The set inverter and ripple filter are matched to the power system by means of three single-phase transformers of 1 kVA with a turn ratio of 1 : 1 to ensure galvanic isolation.

To determine the reference voltage of the active filter, the control scheme shown in Fig. 6 was used. The input signals were the phase voltage vector measured at the load side and the source current vector whose components are the three line currents. Fig. 5 shows the position measure sensors of the voltage and current. The low-pass filters are implemented with a Simulink block. This block is the model of a second-order filter where the cutoff frequency was fixed to 100 Hz and the damping factor was fixed to 0.707. It reaches a settling time of 8 ms.

The control strategy was implemented in a control and general application data acquisition card compatible with MATLAB/Simulink and developed by dSPACE. dSPACE Real Time Interface, together with MathWorks Real Time Workshop, automatically generates real-time code. It allows the processor board to be programmed and I/O boards to be selected. It is based on the DS1005 PPC placed in a dSPACE expansion box. The input board was the dSPACE DS2004 A/D board, and the output board was the DS 51001 DWO. The control board has a PowerPC 750GX processor running at 1 GHz. For the developed experimental prototype, the sampling rate was limited to 50 μs in order to avoid overrun errors.

On the other hand, a hysteresis band control was developed. This pulse width modulation control technique is adequate for applications with APFs; the converter IGBT gating signals are generated comparing the reference signal with the inverter output voltage considering a hysteresis band. Thus, a transistor switches when the error exceeds a fixed magnitude: the

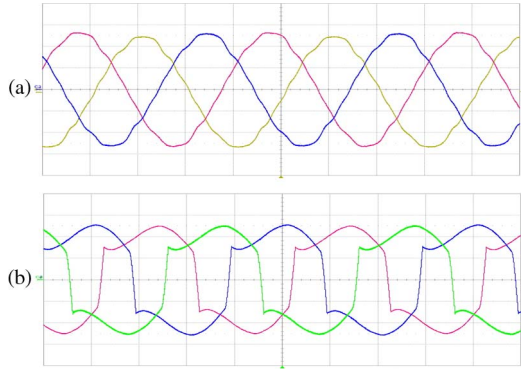


Fig. 7. Load without compensation: (a) Voltage at the PCC and (b) source currents. 120 V/div; 4 A/div; 5 ms/div.

hysteresis band. In this control type, the switching frequency is variable, although in our design, this frequency was limited to 20 kHz to not reach the IGBT maximum switching frequency.

The passive filter is constituted by two LC branches tuned to the fifth and seventh harmonics. The branch tuned to the harmonic of order 5 consists of an inductor of 13.5 mH and a capacitor of 30 μF. The branch tuned to the seventh harmonic is formed by an inductor of 6.75 mH and a capacitor of 30 μF.

IV. EXPERIMENTAL RESULTS

To demonstrate the validity of the proposed control strategy, the experimental prototype (Fig. 5) was subjected to different tests. The compensation equipment was connected to various nonlinear loads. Here, the results of only two loads are presented:

- 1) HCS with four wires;
- 2) HVS with three wires.

These are chosen because they represent two different load kinds, with three or four wires.

These loads have been connected directly to the power grid, of 400 V and 50 Hz.

A. HCS Load

The HCS load consists of three uncontrolled single-phase rectifiers connected between the phase and neutral wire. At the dc side, a 25-Ω resistance in series with a 55-mH inductance is connected.

Fig. 7 shows the waveforms of the source current and the voltage at the PCC before compensation. The source current has an rms value of 7.8 A with a total harmonic distortion (THD) value of 25.3%. The system presents a slight imbalance in the currents as it is shown in Fig. 7(b). This is due to the tolerance in the values of the passive elements connected at the dc side of the rectifier. With respect to the phase voltage at the PCC, the rms value is 218.0 V, and the THD value is 2.7%.

When the passive filter tuned to the fifth and seventh harmonics was connected, the waveforms shown in Fig. 8 were measured. The rms value and the THD value of the source current were 7.9 A and 26.4%, respectively. The waveform currents present a THD higher than that without the passive filter. It is due to the increase of the third-order harmonic which

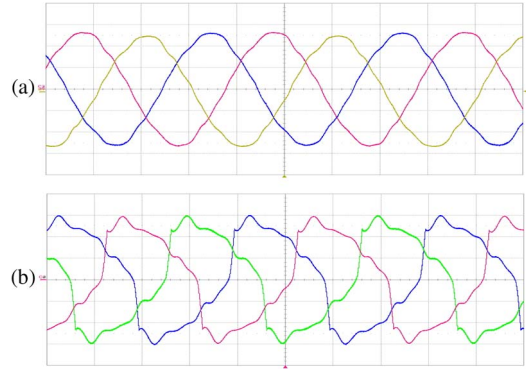


Fig. 8. System with a passive filter: (a) Voltages at the PCC and (b) source currents. 120 V/div; 4 A/div; 5 ms/div.

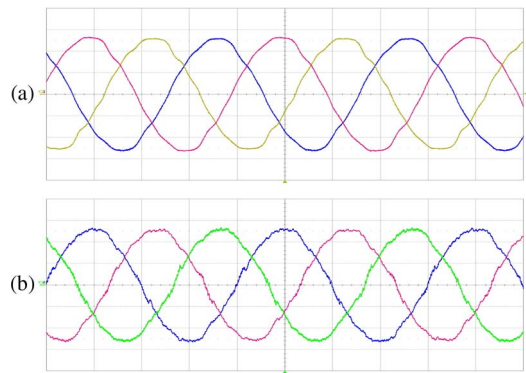


Fig. 9. System with SAPPF: (a) Voltages at the PCC and (b) source currents. 120 V/div; 4 A/div; 5 ms/div.

TABLE I
MEASURED RESULTS (PHASE a): (1) WITHOUT FILTERS, (2) WITH THE PASSIVE FILTER, AND (3) WITH SAPPF

	THD(%)	RMS	H1	H3	H5	H7	H9	P(kW)	Q(kvar)	S(kVA)	PF
⊖	V	2.7	218	218	1.8	3.2	0.2	1.6	0.40 (Ind)	1.7	0.94
	I	25.3	7.8	7.5	1.4	0.9	0.6				
	I _N		4.6	0.2	4.3	0	0.1				
⊖	V	3.3	218	218	2.3	5.1	1.8	1.64	0.41 (Cap)	1.74	0.94
	I	26.4	7.9	7.6	1.7	0.6	0.3				
	I _N		4.7	0.2	4.6	0	0				
⊖	V	2.9	221	221	1.6	3.5	2.3	1.66	0.05	1.66	0.99
	I	3.5	7.5	7.5	0.1	0.1	0.1				
	I _N		0.2	0.2	0.1	0	0				

changes from 1.4 to 1.7. The voltage measured at the PCC was 218 V of rms value and 3.3% of THD value.

When active and passive filters were connected, the waveforms shown in Fig. 9 were measured. The voltages at the PCC and the source currents have practically sinusoidal waveforms. The first one had an rms value of 221 V and a THD value of 2.9%, while the second one had an rms value of 7.5 A and a THD value of 3.5%.

Table I summarizes the most important results. Harmonics, THD, powers, and power factors are included. Only the results for phase “a” are shown. These values were measured with the network analyzer Fluke 434. The power column P shows how the power consumed by the set is slightly higher when the compensation equipment is connected. This is mainly due to the consumption of the passive filter. On the other hand, the

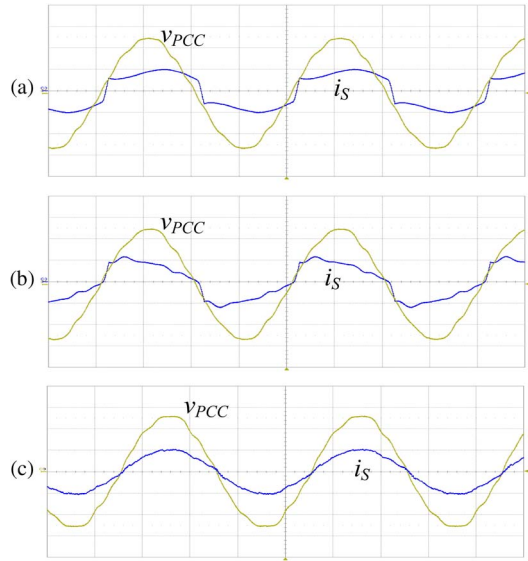


Fig. 10. Voltage at the PCC (v_{PCC}) and source current (i_S); phase α : (a) Without compensation, (b) with the passive filter, and (c) with SAPPF. 120 V/div; 10 A/div; 5 ms/div.

apparent power of the active filter is 0.24 kVA, representing approximately 15% of the apparent power of the load.

Regarding the performance of each of the subsystems of the compensation equipment, that is, the passive filter and the APF, it is interesting to note the following. The passive filter does not compensate the reactive power, so it ranges from an inductive reactive power of 0.40 kvar to a capacitive reactive power of 0.41 kvar when it is connected. The passive filter was not designed to compensate the reactive power.

On the other hand, the active filter is able to reduce the THD due to the improvement of the filtering characteristic of the passive filter. As it is seen in Table I, the fifth-order harmonic of the source current has an rms value of 0.9 A with the system without compensation, and when the passive filter is connected, it is reduced to 0.6 A. However, the active filter is able to improve significantly the filtering characteristic of the passive filter, since it mitigates the source current harmonics.

Fig. 10 shows the waveforms of the voltage at the PCC and the source current before the compensation, with the passive filter connected, and with the active and passive filters connected. It is observed that the source current is sinusoidal and remains in phase with the voltage at the PCC when the hybrid compensator is connected.

On the other hand, the neutral current is reduced from 4.6 to 0.2 A when the compensation equipment is connected. It is due to the reduction of the third and ninth harmonics.

B. HVS Load

The HVS load consists of a three-phase rectifier with a capacitor of 2200 μF in parallel with a resistor of 75 Ω connected at the dc side.

The voltage and current waveforms before the compensation are shown in Fig. 11(a). The voltage THD is 2.5%, and the current THD is 47.7%. The voltage rms value is 218 V, and the current rms value is 6.1 A.

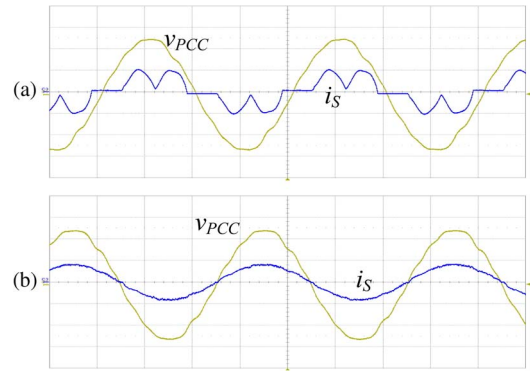


Fig. 11. Voltage at the PCC (v_{PCC}) and source current (i_S); phase α : (a) Without compensation and (b) with SAPPF. 120 V/div; 10 A/div; 5 ms/div.

TABLE II
MEASURED RESULTS (PHASE α): (1) WITHOUT FILTERS, (2) WITH THE PASSIVE FILTER, AND (3) WITH SAPPF

	THD(%)	RMS	H1	H3	H5	H7	H9	P(kW)	Q(kvar)	S(kVA)	PF
①	V	2.5	218	218	0.8	2.6	3.1	1.21	0.14 (Ind)	1.33	0.91
	I	47.7	6.1	5.5	0.1	2.5	0.7				
②	V	3	219	219	0.6	3.4	3.5	1.25	0.67 (Cap)	1.51	0.83
	I	32.8	6.9	6.5	0.2	1.9	0.8				
③	V	2.7	218	218	0.8	2.5	3	1.27	0.01	1.27	1
	I	3.1	5.8	5.9	0	0.1	0.1				

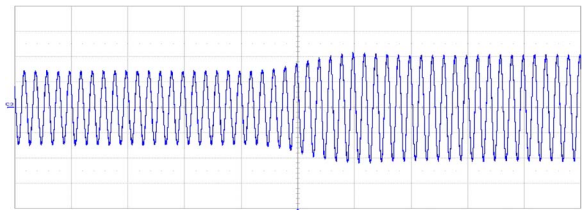


Fig. 12. Source current waveform when a change in the load occurs. 5 A/div; 5 ms/div.

The active, reactive, and apparent powers transferred per phase are $P = 1.21$ kW, $Q = 0.14$ kvar, and $S = 1.33$ kVA, respectively. The load is working with an inductive power factor of 0.91.

Fig. 11(b) shows the voltage waveform at the PCC and the source current after connecting SAPPF. The voltage THD is 2.7%, and the current THD is 3.1%. These values represent a significant improvement of the voltage THD and the current THD. The rms value of the voltage is 218 V, and the rms value of the current is 5.8 A.

Table II summarizes the most important results. The active, reactive, and apparent powers transferred by the set load/SAPPF are 1.27 kW, 0.01 kvar, and 1.27 kVA, respectively. The active power increases due to the consumption of the passive filter coils. The power factor is nearly unity.

The apparent power of the active filter was 0.15 kVA per phase.

On the other hand, it is interesting to verify the behavior of the compensation equipment when a sudden change of load happens. Therefore, Fig. 12 shows the current waveform when the resistance at the dc side of the three-phase rectifier changes from 150 to 75 Ω . For this load, this demonstrates the stability of the system and how the response time is around 5 cycles.

For other load conditions, various tests were carried out for a time delay of 50 μ s. For loads with equivalent resistance between 5 and 107 Ω , the system had a stable behavior. In this section, practical loads have an equivalent resistance of 29.5 Ω for the HCS load and 37.7 Ω for the HVS load.

V. CONCLUSION

In this paper, a control strategy for a hybrid filter constituted by a series active filter and a shunt passive filter has been developed. This strategy was based on optimizing the power transfer between the source and load. By applying the Lagrange multipliers, the value of the equivalent resistance of the set load compensator was determined in order to achieve unity power factor. The approach of this strategy was carried out according to the approach of a multiconductor system to be retrofitted to an active filter of three branches.

Finally, an experimental prototype was designed, and the practical results for a balanced four-wire nonlinear load of HCS type and a balanced three-wire nonlinear load of HVS type were presented. The results obtained allowed the resistive behavior of the set load compensator to be verified. Therefore, with the strategy proposed, it was possible to mitigate the source current harmonics and to compensate the load reactive power.

REFERENCES

- [1] F. Z. Peng and D. J. Adams, "Harmonics sources and filtering approaches," in *Conf. Rec. IEEE IAS Annu. Meeting*, Oct. 1999, vol. 1, pp. 448–455.
- [2] H. Akagi, "Active harmonic filters," *Proc. IEEE*, vol. 93, no. 12, pp. 2128–2141, Dec. 2005.
- [3] Z. Wang, Q. Wang, W. Yao, and J. Liu, "A series active power filter adopting hybrid control approach," *IEEE Trans. Power Electron.*, vol. 16, no. 3, pp. 301–310, May 2001.
- [4] Y. S. Kim, J. S. Kim, and S. H. Ko, "Three-phase three-wire series active power filter, which compensates for harmonics and reactive power," *Proc. IEE—Elect. Power Appl.*, vol. 151, no. 3, pp. 276–282, May 2004.
- [5] Q. Trinh and H. Lee, "An advanced current control strategy for three-phase shunt active power filters," *IEEE Trans. Ind. Electron.*, vol. 60, no. 12, pp. 5400–5410, Dec. 2013.
- [6] A. Bhattacharya and C. Chakraborty, "A shunt active power filter with enhanced performance using ANN-based predictive and adaptive controllers," *IEEE Trans. Power Electron.*, vol. 58, no. 2, pp. 421–428, Feb. 2011.
- [7] K. H. Kwan, P. L. So, and Y. C. Chu, "An output regulation-based unified power quality conditioner with Kalman filters," *IEEE Trans. Ind. Electron.*, vol. 59, no. 11, pp. 4248–4262, Nov. 2012.
- [8] M. Kesler and E. Ozdemir, "Synchronous-reference-frame-based control method for UPQC under unbalanced and distorted load conditions," *IEEE Trans. Ind. Electron.*, vol. 58, no. 9, pp. 3967–3975, Sep. 2011.
- [9] A. Varschavsky, J. Dixon, M. Rotella, and L. Morán, "Cascaded nine-level inverter for hybrid-series active power filter, using industrial controller," *IEEE Trans. Ind. Electron.*, vol. 57, no. 8, pp. 2761–2767, Aug. 2010.
- [10] J. Tian, Q. Chen, and B. Xie, "Series hybrid active power filter based on controllable harmonic impedance," *IET Power Electron.*, vol. 5, no. 1, pp. 142–148, Jan. 2012.
- [11] A. Zobaa, "Optimal multiobjective design of hybrid active power filters considering a distorted environments," *IEEE Trans. Ind. Electron.*, vol. 61, no. 1, pp. 107–114, Jan. 2013.
- [12] V. F. Corasaniti, M. B. Barbieri, P. L. Arnera, and M. I. Valla, "Hybrid active filter for reactive and harmonics compensation in a distribution network," *IEEE Trans. Ind. Electron.*, vol. 56, no. 3, pp. 670–677, Mar. 2009.
- [13] A. Luo, Z. Shuai, W. Zhu, R. Fan, and C. Tu, "Development of hybrid active power filter based on the adaptive fuzzy dividing frequency-control method," *IEEE Trans. Power Del.*, vol. 24, no. 1, pp. 424–432, Jan. 2009.
- [14] F. Z. Peng, H. Akagi, and A. Nabae, "A new approach to harmonic compensation in power systems—A combined system of shunt passive and series active filters," *IEEE Trans. Ind. Appl.*, vol. 26, no. 6, pp. 983–990, Nov./Dec. 1990.
- [15] D. Rivas, L. Moran, J. W. Dixon, and J. R. Espinoza, "Improving passive filter compensation performance with active techniques," *IEEE Trans. Ind. Electron.*, vol. 50, no. 1, pp. 161–170, Feb. 2003.
- [16] S. P. Litrán and P. Salmerón, "Analysis and design of different control strategies of hybrid active power filter based on the state model," *IET Power Electron.*, vol. 5, no. 8, pp. 1341–1350, Sep. 2012.
- [17] P. Salmerón and S. P. Litrán, "A control strategy for hybrid power filter to compensate four-wires three-phase systems," *IEEE Trans. Power Electron.*, vol. 25, no. 7, pp. 1923–1931, Jul. 2010.
- [18] R. S. Herrera and P. Salmerón, "Instantaneous reactive power theory: A reference in the nonlinear loads compensation," *IEEE Trans. Ind. Electron.*, vol. 56, no. 6, pp. 2015–2022, Jun. 2009.
- [19] G. Superti-Furga and G. Todeschini, "Discussion on instantaneous $p-q$ strategies for control of active filters," *IEEE Trans. Power Electron.*, vol. 23, no. 4, pp. 1945–1955, Jul. 2008.
- [20] M. Depenbrock, "Quantities of a multiterminal circuit determined on the basis of Kirchhoff's laws," in *Proc. 4th Int. Workshop Power Definitions Meas. Under Non-Sinusoidal Conditions*, Cagliari, Italy, 1997, pp. 29–35.



Salvador P. Litrán was born in Sanlúcar de Barrameda, Spain. He received the B.Sc. degree in automation and industrial electronics engineering from the University of Seville, Seville, Spain, in 2002, and the Ph.D. degree in electrical engineering from the University of Huelva, Huelva, Spain, in 2011.

He is currently a Professor with and the Head of the Department of Electrical Engineering, Escuela Técnica Superior de Ingeniería, University of Huelva. His research interests include applications of power electronics in distribution systems, power quality analysis, active power filters, hybrid power filters, and renewable energy.



Patricio Salmerón was born in Huelva, Spain. He received the Ph.D. degree from the Department of Electrical Engineering, University of Seville, Seville, Spain, in 1993.

In 1983, he joined the University of Seville as an Assistant Professor with the Department of Electrical Engineering, where he then became an Associate Professor. Since 1993, he has been a Full Professor with the Escuela Técnica Superior de Ingeniería, University of Huelva, Huelva, Spain. He is the Head of the research group Electrical and Electronics of La Rabida, GEYER. He has joined various projects in connection with research on power theory of nonsinusoidal systems and power control in electrical systems. His research interests include electrical power theory, electrical power systems, active power filters, and power conversion systems.